Improved Trajectories in C-Arm Computed Tomography for Non-Circular Fields of View

Magdalena Herbst, Frank Schebesch, Martin Berger, Rebecca Fahrig, Joachim Hornegger and Andreas Maier

***Abstract*—In C-arm computed tomography, the field of view (FOV) is often not sufficient to acquire certain anatomical structures, e.g. a full hip or thorax. Recently proposed methods to extend the FOV use a fixed detector displacement and a 360° scan range to double the radius of the FOV. These trajectories are designed for circular FOVs. However, there are cases in which the required FOV is not circular but rather an ellipsoid. In this work, we show that the use of a dynamically adjusting detector offset can reduce the required scan range when using a non-circular FOV. Furthermore, we present an algorithmic approach which determines the minimal required scan ranges for arbitrary FOVs given a certain detector size. Our results indicate a promising reduction of the necessary scan range especially for ellipsoidal objects. Additionally initial reconstruction results of our method yielded comparable results as when using a fixed detector offset with a full 360° rotation.**

I. Introduction

In computed tomography (CT), the maximum size of the reconstructable field of view (FOV) is a relevant factor. The diameter of a C-arm CT's FOV is typically determined by its detector size and might therefore be limited. Thus, it might be too small to cover certain anatomical areas of interest as for example the hip, the chest or both knees simultaneously.

One solution to increase the FOV is to displace the detector array and adjust the scan range accordingly [1], [2], [3]. The maximal radius of the FOV can be doubled if a displacement of half the detector range is used. Consequently, only half of the extended FOV is acquired with a single projection. Prior to reconstruction these truncated projections are then rebinned to a complete data set which covers the fully extended FOV. One drawback of these methods is, that a full 360° scan range is required to sample the extended FOV completely. Conventional C-arm CT scanners typically do not allow for such high scan ranges and even state-of-the-art robot-mounted systems might not be able to use a 360° scan range in certain angulations. This might be due to an irregular patient position as for example when scanning knees under weight-bearing conditions [4], [5].

Currently these trajectories and their reconstruction methods are designed for circular FOVs, but many anatomical structures may be better described by a non-circular boundary, for example by using ellipses. In this work, we propose a numerical approach that determines the minimally required scan range for arbitrary shaped FOVs, given a certain detector size.

Magdalena Herbst, Frank Schebesch, Martin Berger, Joachim Hornegger, and Andreas Maier are with the Pattern Recognition Lab, Department of Computer Science, Friedrich-Alexander-Universität Erlangen-Nürnberg. Joachim Hornegger and Andreas Maier are with Erlangen Graduate School in Advanced Optical Technologies (SAOT). Rebecca Fahrig is with the Department of Radiology, Stanford University, Stanford, CA, USA.

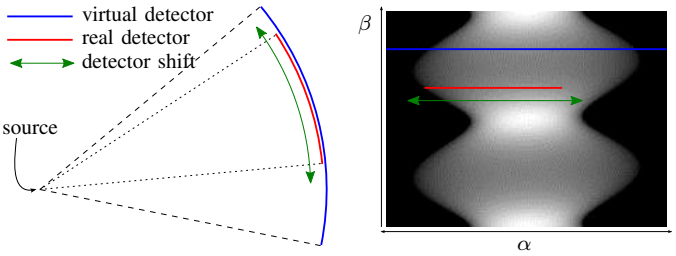

Fig. 1: Rotation of detector around source equals shift of the detector in the sinogram

II. Materials and Methods

A. Correspondences in the Sinogram

In a sinogram of a complete rotation, i.e. a scan range of 360°, every ray is detected twice [6]. These rays are also known as complementary rays. The corresponding line integrals resulting of the complementary rays are equal and their position in the sinogram can be described by the relation

$$f(\alpha, \beta) = f(-\alpha, \beta + \pi + 2\alpha) \ . \tag{1}$$

B. Proposed Algorithm

Subsequently, we consider simple objects that are used to represent various shapes of possible FOVs. For example ellipsoids could be used to represent an outline of a hip slice, or two circles that are positioned off-center could be a suitable FOV for a cross-section of two knees. Now we define a virtual detector that is large enough to cover the whole object such that none of the acquired projections suffer from data truncation. Then a ground truth sinogram is generated using the defined FOV model and an arbitrary but non-zero density distribution within the FOV. For simplicity we assume a constant density over the entire FOV and use the mean density value of water. If the object has non-uniform diameters, e.g. like an ellipse, it is visible in the sinogram that there are line integrals that do not intersect the object, i.e. their sum is zero (cf. Fig. 1, right side). That means that this data is not necessary for reconstruction. Consequently, the idea is to move the detector in such a way that only non-zero line integrals are collected in each projection.

This motion of the detector is illustrated in Fig. 1. The projection of a single angle taken with the virtual detector is depicted by the blue line and represents a single line of the sinogram. The red line represents the real detector and its corresponding data in the sinogram. Moving the red line in the sinogram to the left and right is equivalent to rotating

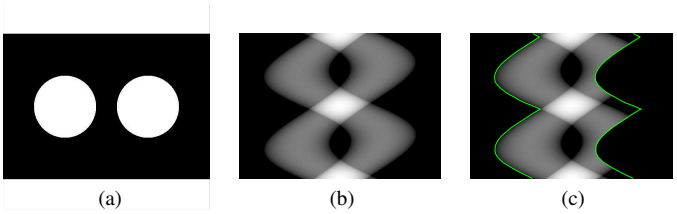

(a) (b) (c)

Fig. 2: Shape of the knees, sinogram of the knees and example for data acquired with a smaller detector with dynamic offset

the real detector while performing the rotation of the whole C-arm system. The rotational movement of the detector can be described with the angle between the central ray of the virtual detector and the central ray of the real detector. It will change while rotating the whole C-arm and can be described as a function of β. In this way, only segments of interest are acquired in the sinogram. The most intuitive way of rotating the detector is to follow the contour of the object in the sinogram (cf. Fig. 2). Hence, a minimal amount of background is scanned. If this movement is performed and a full data set should be acquired, the following constraints have to be fulfilled:

- First, the detector has to be large enough to cover the data for a rotation angle where the object outline is narrowest.
- Second, the detector has to be at least as wide as half of the object outline's widest position in the sinogram. Otherwise the object can not be covered with an off-center acquisition.

If the detector size given by the first requirement is equal to the detector size given by the second requirement, we would have a circular FOV and could use a static off-centered detector with a 360° scan range. In case the first requirement leads to a smaller detector size than the second requirement, we can use the proposed dynamic detector offset to reduce the scan range necessary for a full data acquisition.

In Fig. 2, we visualize the proposed detector motion by a simple example. Fig. 2(a) shows an object that represents the cross section of the shape of two knees by using two uniform circles. Fig. 2(b) depicts the full virtual sinogram of the object and Fig. 2(c) shows the data that is acquired if the proposed movement of the detector is realized. The superimposed lines represent the sinogram boundaries of the rotated detector.

C. Determining the Minimally Required Scan Range

In order to check whether the acquired data is sufficient for reconstruction, at first the truncated sinogram is completed by using the approach described in Algorithm 1. First, the actually acquired projection data is written into the sinogram. Positions in the sinogram which have a value of zero are assumed to be missing rays. Next, these are filled by their corresponding rays given by the redundancy condition Eq. (1). After this completion step, the sinogram is compared to the ground truth. If some data is still missing, the acquired data set is not complete. If there are no differences between the completed sinogram and the ground truth, the acquired data set is complete and therefore sufficient to perform the reconstruction.

Algorithm 1 Sinogram Completion

```
for all (α, β) do
    if f(α, β) was acquired with the trajectory then
        f(α, β) = f(α, β)
    else
        f(α, β) = f(−α, β + π + 2α)
        interpolation is required in this step
    end if
end for
```

We now focus on the derivation of a numerical approach to determine the minimal scan range such that the virtually extended sinogram is still complete. The proposed algorithm to solve this problem is presented in Algorithm 2. To determine the minimally required scan range $\Delta\beta_{min}$ for an arbitrary FOV and a given detector size, we perform a grid search over all possible starting angles $\beta_{Start} \in [0^\circ, 360^\circ]$ and over all possible scan ranges $\Delta\beta \in [180^\circ, 360^\circ]$. First, the minimally required rotation for every starting point is determined by starting with a small $\Delta\beta$. Then we increase it until the data set is complete. Next, the overall minimal $\Delta\beta$ and the corresponding β_{Start} is chosen as a final result. For the step size in angular direction, the angular spacing between the generated projections is used, which also limits the accuracy of the determined minimum scan range.

Subsequently, we present a selection of scanning configurations for the example depicted in Fig. 2. Fig. 3 shows an incomplete configuration with $\beta \in [53^\circ, 299^\circ]$. Fig. 3(a) shows the acquired sinogram, Fig. 3(b) shows the sinogram after the completion step using Algorithm 1 and the white areas in Fig. 3(c) depict the detected missing rays. The two missing areas correspond to each other by Eq. (1), thus, to fill the missing areas it is sufficient to acquire only one of them.

Algorithm 2 Find the minimal complete set for given object and detector size

```
Δβ_min = ∞
β_Start,min = 0
for all β_Start do
    Δβ = 180°
    while data set is not complete do
        Acquire data with β_Start and Δβ
        Complete sinogram with Algorithm 1
        if data set is complete then
            if Δβ < Δβ_min then
                Save the values for the new minimal set:
                Δβ_min = Δβ and β_Start,min = β_Start
            end if
        else
            Increase Δβ
        end if
    end while
end for
```

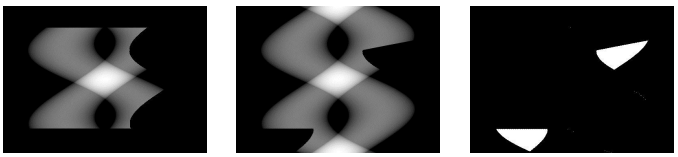

(a) (b) (c)

Fig. 3: Acquired data is not sufficient for a complete data set.

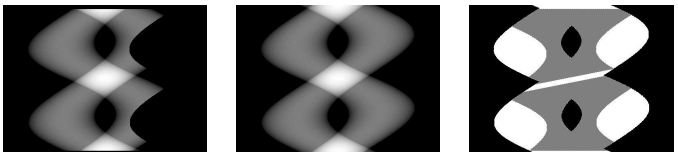

(a) (b) (c)

Fig. 4: More data acquired than the minimal complete data set.

In this configuration, the detector follows the left boundary in the sinogram. Because of this the range of β has to be extended towards the bottom of the sinogram until the lower of the two missing areas is covered completely.

Fig. 4 shows a scanning configuration with $\beta \in [10°, 357°]$. Here, more than the minimal complete data set is acquired. Fig. 4(a) shows the acquired sinogram, Fig. 4(b) shows the sinogram after completion and the gray areas in Fig. 4(c) depict the redundantly acquired data. The range of β could be reduced in the upper part of the sinogram.

In Fig. 5 a minimal complete data set with a scan range of $\beta \in [53°, 357°]$ is shown. Fig. 5(a) shows the acquired sinogram, Fig. 5(b) shows the resulting completed sinogram and Fig. 5(c) shows the acquired redundant areas. With this configuration, there are no missing parts and no redundant areas that can be left out without loosing data that is required for the complete data set.

All algorithms were implemented using CONRAD, an open source software for simulation and reconstruction of CT data (see [7]).

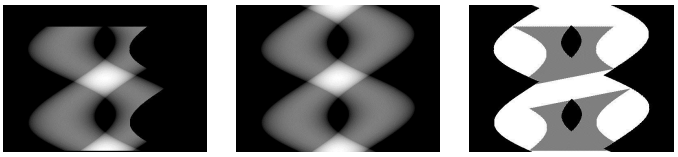

(a) (b) (c)

Fig. 5: Exactly the minimal complete data set is acquired.

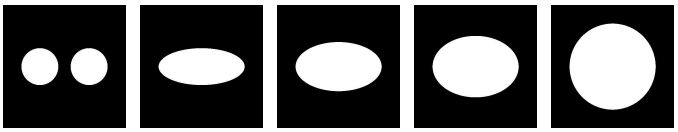

(a) (b) (c) (d) (e)

Fig. 6: Different shapes

Object	Diameter in x-direction	Diameter in y-direction
Two circles	358.4 mm	153.6 mm
Ellipse 1	358.4 mm	153.6 mm
Ellipse 2	358.4 mm	204.8 mm
Ellipse 3	358.4 mm	256 mm
Circle	358.4 mm	358.4 mm

TABLE I: Dimensions of the different objects

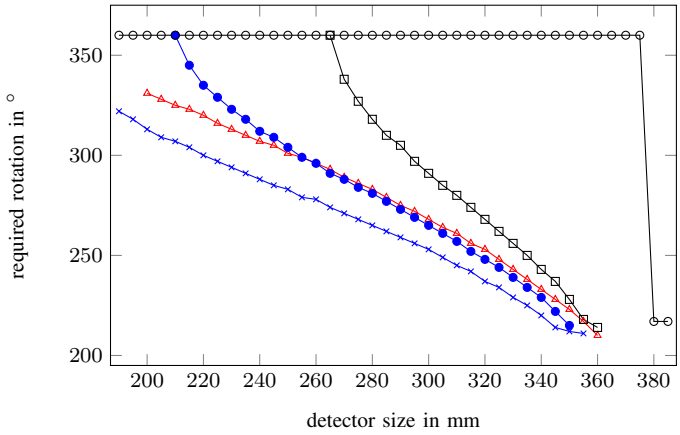

Fig. 7: Required rotation for different objects and detector sizes. Two Circles (—△—), Ellipse 1 (—×—), Ellipse 2 (—●—), Ellipse 3 (—□—), Circle (—○—)

III. Evaluation and Results

A. Evaluation

In Fig. 6 we show the different FOVs that were used for evaluation of the minimally required scan range for different detector sizes. Fig. 6 shows the off-center circles introduced above, Fig. 6(b) to Fig. 6(d) depict ellipses with varying diameter in y-direction and Fig. 6(d) shows a uniform circle. For detailed parameters of the shapes we refer to TABLE I. For our simulations we generated 360 projections for the full scan using an angular increment of $1°$. The focal length was set to $574\,\mathrm{mm}$ and the virtual detector had 501 elements with a spacing of $1\,\mathrm{mm}$ leading to a virtual fan angle of approximately $47°$.

B. Results

Fig. 7 shows the required rotation depending on the detector size for the different objects. For non-circular objects the graphs clearly depict the connection between detector size used and the minimally required scan range. Further we can see that a reduction of the FOV in one direction also reduces the minimally required scan range when the detector size is fixed. At the point where the detector size is greater than the large diameter of the FOV, the trajectory degenerates to a normal short scan approach. For the uniform circle only two possibilities exist. In case the detector is big enough to cover the circle, then a normal short scan [8] is sufficient. If the detector is too small for the circle, a full $360°$ scan range needs to be acquired. For objects that have different dimensions in

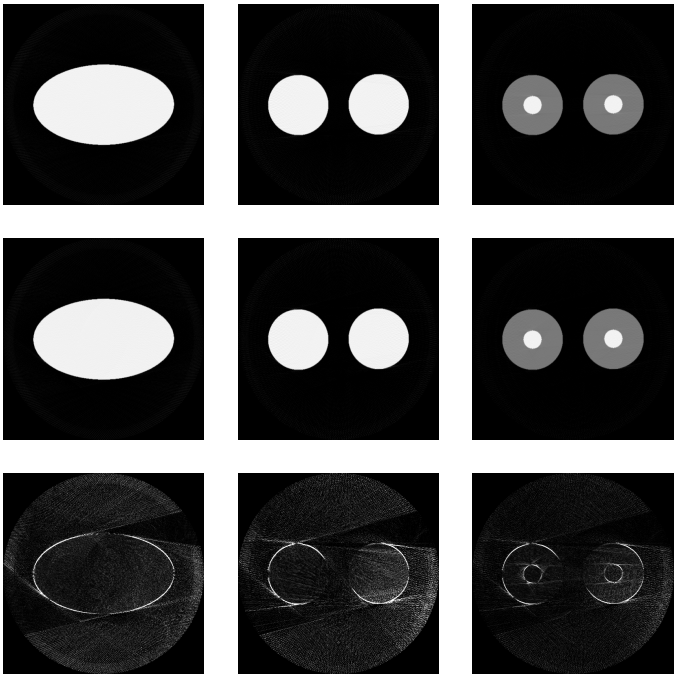

Fig. 8: Reconstruction results, top: reconstruction of the original sinogram, middle: reconstruction of the trajectory result, bottom: difference images. The gray scale window for the reconstruction results is $[0, 1.05]$ and for the difference images $[0, 0.05]$. The maximal difference for the ellipse is 0.232, for the two circles 0.256 and for the modified two circles 0.125.

x- and y-direction, a smaller rotation range is sufficient for a complete data set compared to a circumscribed circular object.

As a proof of concept of our approach, we conducted image reconstructions. First we reconstructed the sinogram using a full 360° scan range, then the rebinned sinogram for the minimally determined scan-range is reconstructed. A visual comparison of both reconstruction results is shown in Fig. 8 for an ellipse and for the object containing two circles. To show that our method is indeed independent of the intensity distributions withing the FOVs we also adjusted the two circles with additional high-density objects in their center. The images show the reconstruction result for the full virtual sinogram (top row), for the minimally complete sinogram (middle row) and the difference image between both of them (bottom row). The reconstruction results of the full virtual sinogram as well as the completed sinogram are in good agreement with each other, showing only minor deviations at the object boundaries. For a quantitative evaluation we also computed the relative root-mean-square-error (rRMSE) for the reconstruction results. We determined an rRMSE of $1.11\,\%$, $1.15\,\%$ and $0.66\,\%$ for the ellipse, the two circle and the modified two circles, respectively.

IV. Discussion

In this work we present a method that is capable to determine the minimally required scan range for extended and arbitrary shaped FOVs given a certain detector size. FOV extensions using a fixed detector displacement produce a circular FOV with the double radius compared to a centered detector [1], [2]. This comes with the cost that projections need to be acquired over a scan range of 360°. Due to space restrictions or limitations given by the scanner geometry, these large scan ranges are sometimes not feasible in an interventional suite. The presented approach, however, enables FOV shapes that are tailored to the actual object and automatically determines the minimally required scan-range to allow for an automatic trajectory planning. We show in Fig. 7 that this can result in a substantial reduction of the required scan range, especially for FOVs that are similar to ellipsoids with different semi-axis lengths.

We assume that the detector is movable throughout the C-arm's global rotation movement, which is already feasible with state-of-the-art C-arm CT scanners. The reconstruction results show that our minimally acquired sinogram achieves an almost identical reconstruction when compared to the reconstruction from the 360° reference sinogram. The difference images in the bottom row of Fig. 8 reveal that most of the deviations are located at the objects' boundaries. We related this to the data completion step where the incomplete sinogram is filled by simple bi-linear interpolation. Thus, inaccuracies are introduced in the sinograms which subsequently leads to the observable loss of spatial resolution in the reconstruction domain. In a yet to be developed online filtered back-projection algorithm, we expect less resolution loss.

In terms of noise we expect the method to be as robust as any filtered back-projection-type reconstruction method. We expect that common noise reduction methods will be applicable with minor modifications [9]. Furthermore, truncation correction can be applied as in any C-arm scan [10].

For future work, we plan to analytically derive a formula that gives the relation between detector size and minimally required scan range. Furthermore, we will investigate the extension to three dimensional FOV shapes.

V. Summary

In C-arm computed tomography, the detector is often too small for the region of interest. Recent trajectories are designed for circular field of views (FOVs). This configuration allows two minimal sets: the short scan and the large volume scan.

For imaging of certain parts of the human body, the required FOV may be non-circular, e.g. for imaging of the thorax, abdomen, or knees. In this paper, we presented a numerical method to investigate scan length vs. detector size in arbitrary objects for fan-beam geometry. We further showed that there exists a continuum of solutions for some non-circular objects and that reconstruction from such trajectories yields image qualities comparable to a full scan acquisition.

References

[1] D. Schäfer and M. Grass, "Cone-beam filtered back-projection for circular X-ray tomography with off-center detector," in *Proceeding of the 10th International Meeting on Fully Three-Dimensional Image Reconstruction in Radiology and Nuclear Medicine, Beijing, PR China*, 2009, pp. 86–89.

[2] H. Kunze and F. Dennerlein, "Cone beam reconstruction with displaced flat panel detector," in *Proceeding of the 10th International Meeting on Fully Three-Dimensional Image Reconstruction in Radiology and Nuclear Medicine, Beijing, PR China*, 2009, pp. 138–141.

[3] G. Wang, "X-ray micro-CT with a displaced detector array," *Medical physics*, vol. 29, no. 7, pp. 1634–1636, 2002.
[4] A. Maier, J.-H. Choi, A. Keil, C. Niebler, M. Sarmiento, A. Fieselmann, G. Gold, S. Delp, and R. Fahrig, "Analysis of vertical and horizontal circular c-arm trajectories," in *SPIE Medical Imaging*. International Society for Optics and Photonics, 2011, pp. 796 123–796 123.
[5] J.-H. Choi, R. Fahrig, A. Keil, T. F. Besier, S. Pal, E. J. McWalter, G. S. Beaupré, and A. Maier, "Fiducial marker-based correction for involuntary motion in weight-bearing C-arm CT scanning of knees. Part I. Numerical model-based optimization," *Medical physics*, vol. 40, no. 9, p. 091905, 2013.
[6] G. L. Zeng, *Medical Image Reconstruction*. Springer, 2010.
[7] A. Maier, H. Hofmann, M. Berger, P. Fischer, C. Schwemmer, H. Wu, K. Müller, J. Hornegger, J.-H. Choi, C. Riess, A. Keil, and R. Fahrig, "CONRAD - A software framework for cone-beam imaging in radiology," *Medical Physics*, vol. 40, no. 11, 2013.
[8] D. L. Parker, "Optimal short scan convolution reconstruction for fan beam CT," *Medical physics*, vol. 9, no. 2, pp. 254–257, 1982.
[9] A. Maier, L. Wigström, H. Hofmann, J. Hornegger, L. Zhu, N. Strobel, and R. Fahrig, "Three-dimensional anisotropic adaptive filtering of projection data for noise reduction in cone beam CT," *Medical Physics*, vol. 38, no. 11, pp. 5896–5909, 2011.
[10] F. Dennerlein and A. Maier, "Region-Of-Interest Reconstruction on medical C-arms with the ATRACT Algorithm," in *Proc. SPIE 8313*, SPIE, Ed., San Diego, California, USA, 2012, pp. 8313–8347.